IEEE Access
Multidisciplinary | Rapid Review | Open Access Journal

Received February 15, 2017, accepted March 1, 2017, date of publication April 24, 2017, date of current version May 17, 2017.

Digital Object Identifier 10.1109/ACCESS.2017.2694608

Statistical Analysis of Surface Texture Performance With Provisions With Uncertainty in Texture Dimensions

FAN MO[1], CONG SHEN[2], JIA ZHOU[1], AND MICHAEL M. KHONSARI[2]
[1]Department of Industrial Engineering, Chongqing University, Chongqing 400044, China
[2]Department of Mechanical and Industrial Engineering, Louisiana State University, Baton Rouge, LA 70803 USA

Corresponding author: Jia Zhou (zhoujia07@gmail.com)

This work was supported by funding from the National Natural Science Foundation of China (Grant 71401018 and Grant 71661167006) and by the Chongqing Municipal Natural Science Foundation (cstc2016jcyjA0406).

ABSTRACT The performance of surface textures with dimensional uncertainty due to the manufacturing process is investigated with statistical models. The uncertainty parameters are geometrical dimensions (i.e., dimple diameter, area ratio, and dimple depth) and the performance parameters include the friction force, the load-carrying capacity, and the coefficient of friction. The results show that logarithmic models provide an excellent fit to the data and can explain more than 99.98% of the variance in data. The most critical geometric parameter for the coefficient of friction and the load-carrying capacity is found to be the dimple diameter, whereas the most critical geometric parameter for the friction force is the area ratio. Manufacturing errors that follow normal distribution with three-sigma quality are found to be insignificant. Under the conditions simulated, it is determined that a dimple diameter of 1883 μm and a dimple depth of 5.5$\sim$6.5 μm yield optimal performance when operating in the hydrodynamic lubrication regime. The area ratio is the key parameter and must be determined based on the requirements of the load-carrying capacity and the coefficient of friction.

INDEX TERMS Dimension uncertainties, parameter optimization, statistical simulation, surface textures.

I. INTRODUCTION

Over the last decade, surface texturing has been identified as an effective method for improving the tribological performance of mechanical parts. It involves manufacturing micro-patterns — such as dimples, grooves, etc. — on contact surfaces in the presence of a lubricating film. These micro-patterns can behave as ''tiny hydrodynamic bearings'' that provide load-carrying support and improve lubrication efficiency [1], [2]. Many micro-machining techniques have been employed to fabricate textured surfaces [3]. Among the available manufacturing techniques, laser surface texturing is by far the most widely used approach since it can be easily applied to different materials [4].

In recent years, a great deal of effort has been devoted to studying the effects of texture's geometric parameters, such as dimple diameter, dimple depth, and the area ratio (the ratio of the textured area and the domain). Both experimental and theoretical research shows that these parameters have a significant effect on tribological performance [5]. Therefore, many studies have been carried out to determine the optimum value of the parameters [6], [7]. Reference [8] provides a survey of papers that focus on the optimization of dimensions in surface texturing to achieve the best performance. This is often achieved by performing an analysis based on specific operating conditions. Ideally, a series of experiments should be conducted to search for the best performance, a process that is time-consuming and expensive due to the large number of tests required.

In most published research on surface texturing, the geometric parameters are considered to be deterministic. However, the dimensions of surface textures vary within certain limits because of manufacturing tolerances [9]. As the thickness of the lubricant film and the size of textures are very small —typically on the order of a micron— uncertainty in the size of the texture dimensions may greatly influence performance. This paper is devoted to the evaluation of surface texture performance with the provision for dimensional uncertainty. The results are also presented to determine the optimized size of a texture based on statistical analyses.

II. UNCERTAINTY OF TEXTURE DIMENSIONS

Texture dimensions are usually not deterministic due to the uncertainty in the manufacturing processes. This uncertainty can be classified into two categories: systematic errors that

are repeatable and reproducible and random errors that vary even when the system is subjected to the same operating conditions. As a result, the texture dimensions usually vary within the manufacturing tolerances.

Previous studies of the uncertainty of manufacturing dimensions have branched out in two directions. One branch of study investigates how uncertainty influences manufacturing performance. The other branch investigates how to set the best manufacturing tolerance of parameters in response to the uncertainty.

Regarding the first branch, a typical application is in gear systems where manufacturing errors result in vibrations. For spur gears, for example, manufacturing errors are simulated by generating a random profile, which fits the gear K-chart [10]. For planetary gear sets, Bodas and Kahraman [11] report how manufacturing errors and assembly variations influence the position of tooth contact surfaces. Consideration is given to static conditions, and only one error is investigated at a time assuming that all other errors are absent. This approach does not provide any information on the interaction among variables. A subsequent study investigated the errors associated with the carrier pinhole position simulated at three fixed levels [12].

Regarding the second branch, the tolerance of parameters —the so-called tuning parameters—are obtained through various optimization methods, the Taguchi method, and the method of imprecision [13], [14]. Including tuning parameters in the design process can result in designs that are more tolerant of variational noise. Analyzing the uncertainty of parameters has become an important part of robust mechanical design [15], [16]. Using the milling process as an example, reference [17] analyzes the deviation between the real surface and the nominal machine surface to determine manufacturing tolerances. This approach has been proven to be useful both in simulation and in practice.

Along with the improvement of machining accuracy, various statistical methods have been proposed to overcome uncertainty. For example, Puh *et al.* [18] investigated the multi-objective optimization of the turning process of an optimal parametric combination to provide the minimum surface roughness with the maximum material removal rate using the Grey-Based Taguchi method. Prasad and Babu [19] applied the analysis of variance (ANOVA) technique to evaluate the significance of parameters on the overall quality characteristics of the cutting process in an uncertain environment. A variety of other methods have been presented for analyzing nonlinear vibrations of spur gears in the presence of manufacturing errors [10], [20]–[22]. Manufacturing errors are treated stochastically, starting from the knowledge of the gear tolerance class.

Although previous studies have considered the uncertainty of texture dimensions, they usually have a number of drawbacks. They are classified in three different categories. (1) *quantifying uncertainty* where many studies used multiple fixed levels, without considering the probability of each level. (2) *mixed uncertainty from multiple sources* where only one variable at a time is investigated, without considering the interaction with other variables. (3) *generalization of uncertainty* where the simulated uncertainty is applied to a specific manufacturing process and operating conditions, and thus it is difficult to generalize the results to other conditions.

In this study, we present an analysis that treats the problem of quantifying uncertainty from multiple sources in a more general fashion and applies the technique to study the performance of textured surfaces. The objective of the research is to investigate the effects of uncertainty of geometrical parameters (dimple diameter d_0, area ratio S_p, and dimple depth h_g) on the performance of surface textures (friction force F, load-carrying capacity W, and coefficient of friction f). The texture shape is considered to be perfectly circular, but the value of dimensions may vary with a certain probability. In order to achieve the above results, the authors first explore the uncertainty of geometrical parameters and then investigate their influence on the performance of surface textures. Statistical models are proposed and the key influential critical geometric parameters are identified.

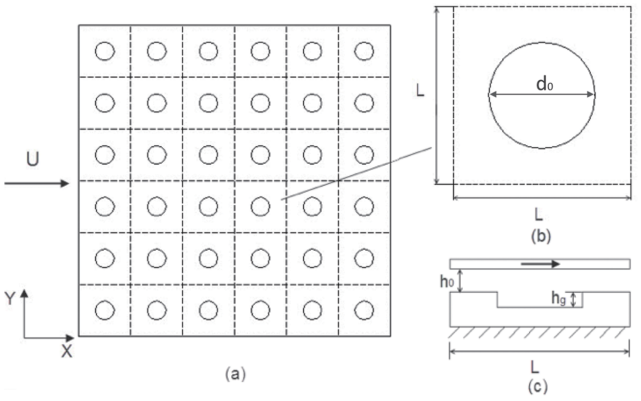

FIGURE 1. Schematic of a textured surface (a) distribution of textures; (b) typical unit cell; (c) side view of a unit cell.

III. STATISTICAL MODEL OF PERFORMANCE OF SURFACE TEXTURES

A. PROBLEM FORMULATION

The schematic of a textured surface is shown in Fig. 1. Each dimple is located at the center of an imaginary square cell of length L. To simplify the simulations, a single unit cell is used as the computational domain [Fig. 1(b)]. Periodic boundary conditions are applied in the sliding direction (X) to account for the interaction between textures, and the boundaries in the other direction (Y) are kept at ambient pressure. The dimple's diameter is denoted by d_0 and its depth is h_g. The area ratio S_p can be calculated by

$$S_p = \frac{\pi d_0^2}{4L^2}. \tag{1}$$

As shown in Fig. 1(c), one of the sliding pairs is stationary and the other slides with a velocity (U). The film thickness

equation in cylindrical coordinates for two regions, one over the asperity and the other in the grooves, is given as

$$h(r) = \begin{cases} h_0, & (d < d_0) \\ h_0 + h_g, & (d_0 \le d \le L) \end{cases} \quad (2)$$

We assume that surfaces are rigid and that the density (ρ) and viscosity (μ) variations across the thin lubricant are negligible. Under the typical thin-film lubrication analyses, the equation governing the hydrodynamic pressure distribution is given by the Reynolds equation

$$\frac{\partial}{\partial x}\left(h^3\frac{\partial p}{\partial x}\right) + \frac{\partial}{\partial y}\left(h^3\frac{\partial p}{\partial y}\right) = 6\mu U\frac{\partial h}{\partial x} \quad (3)$$

Equation (3) is solved based on the given film profile and boundary conditions. The details are given in reference [31]. To non-dimensionalize the friction force (F) and the load-carrying capacity (W) the following dimensionless terms are defined:

$$\bar{F} = \frac{F}{P_a(d_0/2)^2} \quad \bar{W} = \frac{W}{P_a(d_0/2)^2} \quad (4)$$

where $\bar{F}$ and $\bar{W}$ are the dimensionless friction force and load-carrying capacity, and P_a is the ambient pressure in the simulation.

B. STATISTICAL MODELING

In a real manufacturing environment, the structure of surface textures is not perfect and dimensions such as the dimple diameter, the dimple depth, and the area ratio differ from the specified design dimensions. Regression models that do not include the variables of manufacturing errors must be explored to obtain a general overview of the efficiency of different regression models. For this purpose, we examine five different categories of models: linear models, quadratic models, cubic models, logarithmic models, and logarithmic cubic models (as given in Table 1). These models are basic and lend themselves to simple regression analyses. Instead of the disturbances/random errors ε_i and the parameters *a, b, c,* and d, we estimate their values from sampled data and obtain the fitted model with the residual ε_i and the parameters $\hat{a}$, $\hat{b}$, $\hat{c}$, and $\hat{d}$.

In order to estimate the parameters in regression models, data for the dimple diameter, the area ratio, the dimple depth, the corresponding friction force, the load-carrying capacity, and the coefficient of friction are required. The data are generated in numerical experiments by solving the appropriate governing equations. The observed values of random texture dimensions are first generated and then used in computer programs to obtain the values of performance parameters by solving the Reynolds equation. Each parameter has a sample of 1000 data from the numerical experiments. Based on this, the parameters in five regression models are estimated to determine the relationship between texture dimensions and performance. Depending on the validity of the models, the authors further add the manufacturing errors of texture dimensions into the models that have high validity.

TABLE 1. Five regression models.

Model Type	Equation
Linear models	$y_i = \hat{a} + \hat{b}X_1 + \hat{c}X_2 + \hat{d}X_3 + \varepsilon_i$
Quadratic models	$y_i = \hat{a} + \hat{b}X_1 + \hat{c}X_2 + \hat{d}X_3 + \hat{e}X_1X_2 + \hat{f}X_2X_3 + \hat{g}X_1X_3 + \hat{h}X_1^2 + \hat{i}X_2^2 + \hat{j}X_3^2 + \varepsilon_i$
Cubic models	$y_i = \hat{a} + \hat{b}X_1 + \hat{c}X_2 + \hat{d}X_3 + \hat{e}X_1X_2 + \hat{f}X_2X_3 + \hat{g}X_1X_3 + \hat{h}X_1^2 + \hat{i}X_2^2 + \hat{j}X_3^2 + \hat{k}X_1^2X_2 + \hat{l}X_1^2X_3 + \hat{m}X_2^2X_1 + \hat{n}X_2^2X_3 + \hat{o}X_3^2X_1 + \hat{p}X_3^2X_2 + \hat{q}X_1X_2X_3 + \hat{r}X_1^3 + \hat{s}X_2^3 + \hat{t}X_3^3 + \varepsilon_i$
Logarithmic models	$lny_i = \hat{a} + \hat{b}X_1 + \hat{c}X_2 + \hat{d}X_3 + \varepsilon_i$
Logarithmic cubic models	$lny_i = \hat{a} + \hat{b}X_1 + \hat{c}X_2 + \hat{d}X_3 + \hat{e}X_1X_2 + \hat{f}X_2X_3 + \hat{g}X_1X_3 + \hat{h}X_1^2 + \hat{i}X_2^2 + \hat{j}X_3^2 + \hat{k}X_1^2X_2 + \hat{l}X_1^2X_3 + \hat{m}X_2^2X_1 + \hat{n}X_2^2X_3 + \hat{o}X_3^2X_1 + \hat{p}X_3^2X_2 + \hat{q}X_1X_2X_3 + \hat{r}X_1^3 + \hat{s}X_2^3 + \hat{t}X_3^3 + \varepsilon_i$

TABLE 2. Data used for the simulation.

Parameter	Value
Minimum film thickness, h_0	5 μm
Lubricant viscosity, μ	0.38 Pa·s
Sliding velocity, U	1 m/s
Cavitation pressure, P_c	100 kPa
Ambient pressure, P_a	100 kPa

IV. METHOD

A. GEOMETRIC PARAMETERS

For better readability, the following parameter definitions are introduced.

x_1 ≅ dimple diameter, d_0.
x_2 ≅ area ratio, S_p.
x_3 ≅ dimple depth, h_g.
e_1 ≅ manufacturing errors of X_1.
e_2 ≅ manufacturing errors of X_2.
e_3 ≅ manufacturing errors of X_3.
y_1 ≅ dimensionless friction force, $\bar{F}$.
y_2 ≅ dimensionless load-carrying capacity, $\bar{W}$.
y_3 ≅ coefficient of friction, f.

The friction force, the load-carrying capacity, and the coefficient of friction are treated as non-dimensional parameters. The texture shape is considered to be perfectly circular, but the values of the dimple diameter, the area ratio, and the dimple depth are assumed to vary with a certain probability. Thus, e_1, e_2, and e_3 are random variables. The working conditions (e.g., sliding velocity U, lubricant viscosity μ, and minimum film thickness h_0) and the length of the square cell (L) are determined. The working conditions are fixed and their values are listed in Table 2.

Table 3 lists some of the preferred geometric parameters reported in the literature. Therefore, the range for textured geometry in the simulations is 100∼2000 μm for the dimple diameter, 5∼30% for the area ratio, and 1∼10 μm for the dimple depth.

TABLE 3. Preferred geometric parameters used in literature.

Author/Year	Testing condition	Shape	Area ratio	Diameter (μm)	Depth (μm)
Ryk 2002 [23]	Steel ring/cast iron liner reciprocating	Circular dimple	13%	100	10
Kovalchenko 2005 [24]	Steel/steel pin on disk	Circular dimple	12%	78	5.5
Galda 2009 [25]	Cast iron/steel block on ring	Circular dimple	12.5%	900	60
Yan 2010 [26]	Chromium coated ring /cast iron ring	Circular dimple	5%	100	10
Grabon 2013 [27]	Piston ring/cast iron liner reciprocating	Circular dimple	13%	150~200	5

B. ASSUMPTIONS

Five main assumptions are as follows. Assumption 1 is to simplify and standardize the surface textures. Assumptions 2, 3, 4, and 5 determine the statistical parameters according to the actual manufacture and operation.

Assumption 1: Type of asperity geometries is a perfect circle.

In a real manufacturing environment, the edge of the dimple is not smooth enough and the type of asperity geometries should be considered as an irregular polygon. However, this research simplifies the shape of the dimple as a perfect circle to focus on the influence of the diameter and depth of the dimple, since these two dimple parameters are widely mentioned in the studies of the performance of surface textures.

Assumption 2: The three geometrical parameters (dimple diameter, area ratio, and dimple depth) are uniformly distributed as specified.

The recommended range for the textured geometry is 100∼2000 μm for the dimple diameter, 5∼30% for the area ratio, and 1∼10 μm for the dimple depth. The value of each texture's geometry is usually determined by the designers' experience; they can set the textured geometry values independently and randomly. Therefore, in this research, the values of texture geometry are randomly picked from their value range, and the possibility to pick each value is equal. That is, x_1, x_2, and x_3 are uniformly distributed.

Assumption 3: The manufacturing errors of three geometrical parameters follow the normal distribution.

The distribution of random texture dimensions is related to the manufacturing process. For example, depending on the characteristics of the manufacturing drill, the dimple size may be random and follow a uniform distribution, or it may follow the normal distribution. No matter what the distribution, according to the central limit theorem, it would be approximately normally distributed for a sufficiently large number. Thus, in this study, it is assumed that the random variables follow the normal distribution.

Assumption 4: The laser texturing reaches three-sigma performance level.

Since three-sigma is a common quality metric in manufacturing and is widely used to set the control limit, the manufacturing errors are expected to follow a normal distribution with the three-sigma quality. That is, e_1, e_2, and e_3 follow the standard normal distribution, and 99.73% of geometrical parameters are within three standard deviations of the mean.

Assumption 5: Manufacturing errors are independent, and the relative tolerance band of e_1, e_2, and e_3 is $\pm 1\%$.

Suppose that e_1, e_2, and e_3 are independent of each other. Those larger than 1% of the designed size or smaller than 1% of the designed size are considered to be defective. That is, e_1, e_2, and e_3 are within the range from 99% to 101% of the average.

C. NUMERICAL EXPERIMENTS

Numerical experiments are used in this research to generate data for texture dimensions and associated manufacturing errors. Since the one-factor-at-a-time strategy fails to consider the interaction between the factors, the factorial design (as given in Table 4) is implemented in the numerical experiments.

TABLE 4. Factorial design of the numerical experiments.

		x_2								
		1			2			3		
		x_3			x_3			x_3		
		1	2	3	1	2	3	1	2	3
x_1	1	$O_{1...}$ [a] O_{125}	$O_{126...}$ O_{250}	$O_{251...}$ O_{375}	$O_{1126...}$ O_{1250}	$O_{1251...}$ O_{1375}	$O_{1376...}$ O_{1500}	$O_{2251...}$ O_{2375}	$O_{2376...}$ O_{2500}	$O_{2501...}$ O_{2625}
	2	$O_{376...}$ O_{500}	$O_{501...}$ O_{625}	$O_{626...}$ O_{750}	$O_{1501...}$ O_{1625}	$O_{1626...}$ O_{1750}	$O_{1751...}$ O_{1875}	$O_{2626...}$ O_{2750}	$O_{2751...}$ O_{2875}	$O_{2876...}$ O_{3000}
	3	$O_{751...}$ O_{875}	$O_{876...}$ O_{1000}	$O_{1001...}$ O_{1125}	$O_{1876...}$ O_{2000}	$O_{2001...}$ O_{2125}	$O_{2126...}$ O_{2250}	$O_{3001...}$ O_{3125}	$O_{3126...}$ O_{3250}	$O_{3251...}$ O_{3375}

[a] O=Observation

Independent variables in the numerical experiments are x_1, x_2, x_3, e_1, e_2, and e_3. x_1, x_2, and x_3 are design variables. Their values can be set randomly within the range. The range of x_1, x_2, and x_3 is equally divided into n proportions. That is, x_1, x_2, and x_3 have $n+1$ levels from the uniform distribution, which could be used for the experiment. Few experiments involve more than four levels per treatment factor [28]; therefore, the research determines three levels for each factor of x_1, x_2, and x_3. That is, $n = 2$, and there are 27 treatments.

The parameters e_1, e_2, and e_3 represent the randomly occurring manufacturing errors that cannot be controlled, so they are assumed to follow the normal distribution with three-sigma quality and a relative tolerance band of $\pm 1\%$. Based on this, N points are chosen from the normal distribution curve of each factor (e_1, e_2, and e_3). The N points can be referred to as replication, which repeats the observations at every level of the factors and increases the sample sizes. Replication permits the experimenter to obtain a more precise estimate of the parameter. Determining five replicates per

factor can produce 125 observations in each treatment (the cell in Table 4), which is deemed to be adequate to ensure accuracy [29]. That is, $N = 5$, and there are 125 observations for each treatment.

In Table 4, there are 3375 observations. They follow the normal distribution. The average value equals each designed value (x_1, x_2, and x_3) and the standard deviation derives from the three-sigma performance level and the tolerance band. R programs are used to generate experimental data.

Dependent variables y_1, y_2, and y_3 are used to measure performance. They are computed based on the real value rather than the designed value of geometrical parameters using the Matlab® program.

V. RESULTS

A. COMPARISON OF DIFFERENT MODELS

In order to select effective models, the abovementioned five statistical models are compared using a sample size of 1000 data obtained from numerical experiments that involve solving the Reynolds equation. Using the results, the statistical parameters of five regression models are calculated.

TABLE 5. Summary of five models for each dependent variable.

	Model type	df^a	R^{2b}	RSE^c
y_1	Linear	996	71.50%	0.357
	Quadratic	990	92.00%	0.189
	Cubic	982	98.00%	0.095
	Logarithmic	996	96.80%	0.104
	Logarithmic cubic	986	99.81%	0.025
y_2	Linear	997	81.60%	0.700
	Quadratic	995	95.40%	0.349
	Cubic	993	98.60%	0.191
	Logarithmic	997	97.20%	0.059
	Logarithmic cubic	992	99.96%	0.007
y_3	Linear	996	76.30%	1.921
	Quadratic	991	91.00%	0.837
	Cubic	982	99.00%	0.391
	Logarithmic	996	96.60%	0.114
	Logarithmic cubic	986	99.84%	0.025

[a]df = degrees of freedom, which refers to the number of values in the final calculation of a statistic that is free to vary.
[b]R^2 = Adjusted R-Squared, which is a modified version of R-squared that has been adjusted for the number of predictors in the model. R-squared refers to how close the data are to the fitted regression line. The larger R^2, the better is the result.
[c]RSE = Residual Standard Error, which is an estimate of the standard deviation, and substantially expresses the variability in the dependent variable "unexplained" by the model. The smaller RSE, the better is the result.

As given in Table 5, the logarithmic cubic model outperforms other models in terms of the highest explained variance (R^2) and the lowest residual standard error (RSE). Although the cubic model has a slightly lower explained variance than the logarithmic cubic model, the cubic model has a higher residual standard error and more terms in the equation.

On the other hand, the logarithmic model is much better than the logarithmic cubic model due to fewer terms. Compared with the logarithmic cubic model although the explained variance is lower and the residual standard error is higher, it is simple and easy to comprehend.

Therefore, the model that best fits the sample data is the logarithmic cubic model; however, the large number of terms makes it difficult to comprehend. Compromising predictive power for comprehension, the logarithmic cubic models are also good-fit models. Accordingly, the authors go on to derive models with manufacturing errors based on the logarithmic model.

B. MODEL WITH MANUFACTURING ERRORS

There are two models derived from the logarithmic model: a model with independent manufacturing errors and a model including interaction with manufacturing errors. In the first model, the authors assume that manufacturing errors are independent (e.g., manufacturing x_1 would not influence x_2 or x_3). In the second model, the authors assume that manufacturing errors are dependent, e.g., with x_1 and x_3 manufactured using the same tool. That is, the first model only considers the interaction between the texture dimensions, and the second model considers the interaction between the texture dimensions and the interaction with manufacturing errors.

TABLE 6. Summary of the model with independent manufacturing errors.

Model	F^a	df	p^b	R^2	RSE
$\ln(\bar{F})$	9.0144×10^6	3367	<0.001	99.9946%	0.005748
$\ln(\bar{W})$	3.3568×10^6	3364	<0.001	99.9900%	0.014191
$\ln(f)$	1.7999×10^6	3364	<0.001	99.9813%	0.018228

[a]F = F-value, which is referred to as the F statistic.
[b]P = p-value, which is defined as the probability of obtaining a result equal to or "more extreme" than what is actually observed, when the null hypothesis is true.

TABLE 7. Summary of the model including interaction with manufacturing errors.

Model	F	df	p	R^2	RSE
$\ln(\bar{F})$	1.1241×10^7	3359	<0.001	99.9980%	0.003517
$\ln(\bar{W})$	2.0305×10^6	3357	<0.001	99.9902%	0.013994
$\ln(f)$	1.2072×10^6	3357	<0.001	99.9836%	0.017071

The results indicate that the first model and the second model can explain 99.98% of the variance independent variables (as given in Table 6 and Table 7). The two models have the comparative power to explain dependent variables. The latter is slightly better in terms of smaller RSE but at the cost of more terms and greater complexity. Therefore, the models with manufacturing errors that only consider the interaction between texture dimensions are used in the subsequent analysis.

The equations of the friction force $\bar{F}$, the load-carrying capacity $\bar{W}$, and the coefficient of friction f are as

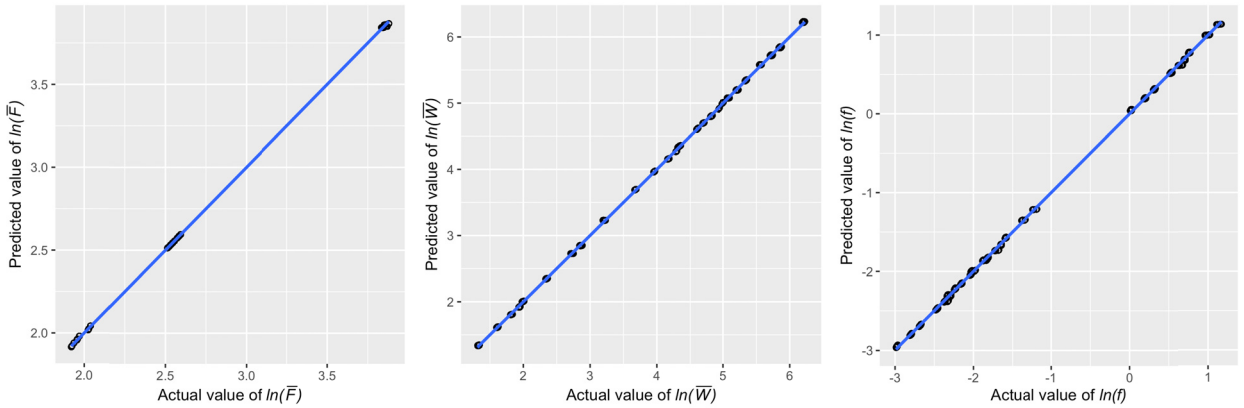

FIGURE 2. The actual value and the predicted value for each performance parameter.

TABLE 8. Results of model fit test.

Model	R^2 ($N = 3375$)	R^2 ($N = 27000$)
$\ln(\bar{F})$	99.99%	99.99%
$\ln(\bar{W})$	99.99%	99.99%
$\ln(f)$	99.98%	99.99%

follows:

$$\begin{aligned} ln\bar{F} &= 4.573217 - 15.25076 \times S_p - 6.009112 \times e_2 \\ &\quad - 5.110964 \times 10^3 \times h_g + 22.72483 \times \mathrm{S}_p \times \mathrm{S}_p \\ &\quad + 4.826932 \times 10^8 \times h_g \times h_g \\ &\quad - 3.871218 \times 10^4 \times S_p \times h_g \qquad (5) \\ ln\bar{W} &= 2.643605 + 3.561460 \times 10^3 \times d_0 \\ &\quad + 5.642161 \times 10^2 \times e_1 - 10.64639 \times S_p \\ &\quad - 2.044102 \times e_2 - 2.509898 \times 10^5 \times h_g \\ &\quad - 7.372122 \times 10^4 \times e_3 - 9.452432 \times 10^5 \times d_0 \\ &\quad \times d_0 + 14.41329 \times \mathrm{S}_p \times \mathrm{S}_p - 2.190898 \times 10^{10} \\ &\quad \times h_g \times h_g + 6.746253 \times 10^4 \times S_p \times h_g \qquad (6) \\ lnf &= 1.929612 - 3.561458 \times 10^3 \times d_0 \\ &\quad - 5.642161 \times 10^2 \times e_1 - 4.604371 \times S_p \\ &\quad - 3.965011 \times e_2 - 2.561008 \times 10^5 \times h_g \\ &\quad + 6.942814 \times 10^4 \times e_3 + 9.452428 \times 10^5 \times d_0 \\ &\quad \times d_0 + 8.311538 \times \mathrm{S}_p \times \mathrm{S}_p + 2.239167 \times 10^{10} \\ &\quad \times h_g \times h_g - 1.061747 \times 10^5 \times S_p \times h_g \qquad (7) \end{aligned}$$

C. MODEL FIT TEST

The models are derived from a data sample with 3375 observations (n = 2 and N = 5). To validate the models, a large sample with 27000 observations is generated (n = 2 and N = 10) and tests with the first model in the above section, which only considers the interaction between texture dimensions. The results of R^2 show that this model has a very good fit with accuracy above 99.98% regardless of the number of observations (as given in Table 8).

To evaluate the model fit, the predicted values of dependent variables and their actual values are compared. As shown in Fig. 2, the predicted value is almost identical to the actual value of each performance parameter. Therefore, the models are predictive.

TABLE 9. The T value in the first model.

	$\ln(\bar{F})$	$\ln(\bar{W})$	$\ln(f)$
d_0	N/A[a]	2854.100	2221.978
e_1	N/A	11.377	8.857
S_p	2877.781	813.742	273.984
e_2	67.686	9.326	14.084
h_g	39.608	787.870	625.864
e_3	N/A	7.219	5.293
R_0^2	N/A	1636.615	1274.139
S_p^2	1595.683	409.947	184.042
h_g^2	44.685	821.535	653.674
$S_p \times h_g$	146.717	103.565	126.894

[a]N/A=Not significant in the model

D. CRITICAL TEXTURE DIMENSIONS

Critical texture dimensions are identified through the most influential parameters in the regression models. Comparing the coefficients of each variable is a good approach to identify critical dimensions. However, the orders of magnitude of variables and their range of variation are different, so it is difficult to compare them by their coefficients. Another approach is to compare the T value of these variables. The T value directly reflects the influence of independent variables on $\ln(\bar{F})$, $\ln(\bar{W})$, and $\ln(f)$, and it is not restricted by the orders of magnitude of variables. The T value of each independent variable in the models is given in Table 9. Based on this, the importance of each independent variable is shown in Fig. 3.

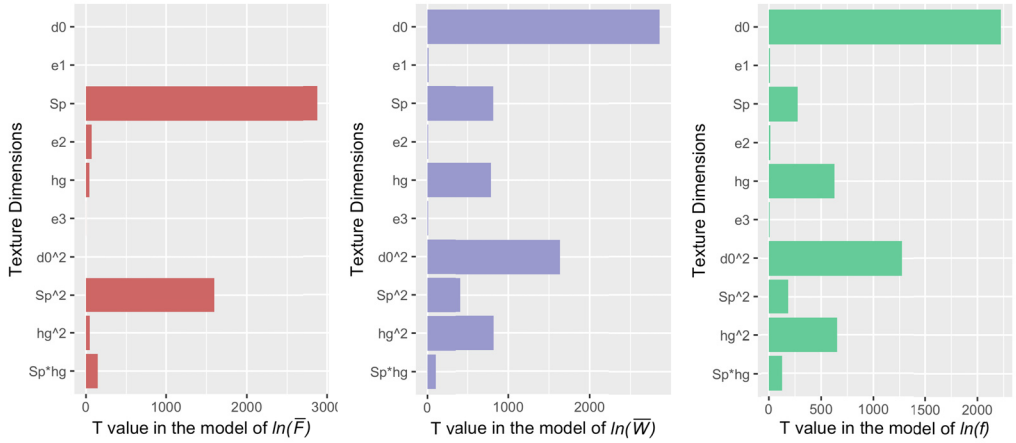

FIGURE 3. The importance of each independent variable in the model.

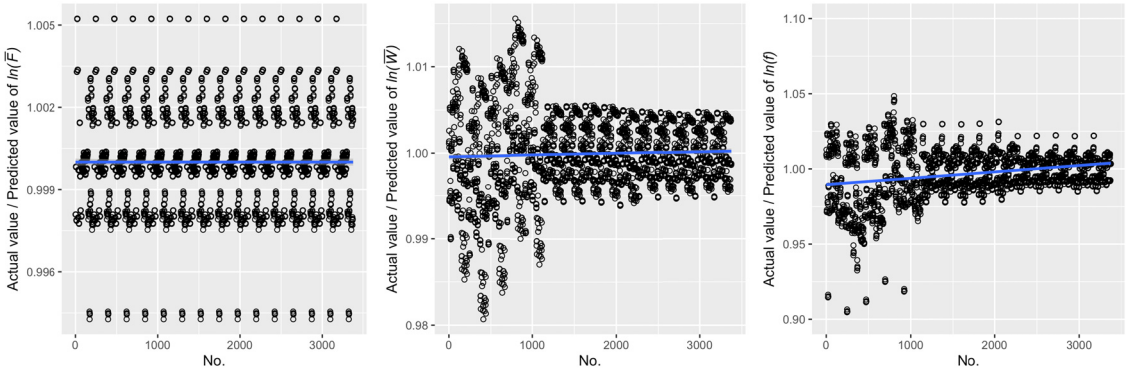

(a) *Residual of model In($\bar{F}$)* (b) *Residual of model In($\bar{W}$)* (c) *Residual of model In(f)*

FIGURE 4. The actual value and the predicted value for each performance parameter.

Geometric factors have a greater influence on the performance of surface textures than their manufacturing errors. Some manufacturing errors also influence performance but their extent of influence is much less. For the friction force $\bar{F}$, the influential manufacturing error is represented by e_2. For the load-carrying capacity $\bar{W}$ and the coefficient of friction f, the manufacturing errors e_1, e_2, and e_3 have comparable influence. However, they have little influence on surface texture performance compared to the dimple diameter, the area ratio, and the dimple depth.

VI. DISCUSSIONS

A. FURTHER ANALYSIS ON THE MODEL FIT

Regression models in the research have a remarkably high model fit and have the capability to predict texture performance. To explore the reasons for the high fit and further evaluate the models, the ratios of actual value and predicted value of texture performance are calculated.

The deviation between the actual value and the predicted value is found to be small. The deviation of ratios is less than 0.01 in terms of the friction force (as shown in Fig. 4a). For the load-carrying capacity and the coefficient of friction, the deviation of ratios is slightly higher but remains less than 0.01 and 0.05, respectively [as shown in Figs. 4(b) and 4(c)]. Some variations of the first third of the samples have not been explained. These samples have a small dimple diameter (i.e., approximately 50 μm), but optimized values of the texture performance call for a large diameter (as mentioned in Table 11). Therefore, the deviations have little influence on the prediction of optimal performance. The models are highly predictive.

B. MODELS WITHOUT MANUFACTURING ERRORS

The analysis of critical texture dimensions reveals that manufacturing errors have little effect on texture performance. As a result, the influence of manufacturing errors is removed in those models. Models of the friction force, the load-carrying capacity and the coefficient of friction without e_1, e_2, and e_3 are then built and compared with those models with e_1, e_2, and e_3.

As shown in Table 10, the value of some statistical parameters shows a small decline, and the decrease of model fit is

TABLE 10. Comparisons between models with *E* and models without *E*.

Model		F	R^2	RSE
$\ln(\bar{F})$	With e	9.0144×10^6	99.9946%	0.005748
	Without e	5.3480×10^6	99.9874%	0.008830
$\ln(\bar{W})$	With e	3.3568×10^6	99.9900%	0.014191
	Without e	3.9834×10^6	99.9894%	0.014565
$\ln(f)$	With e	1.7999×10^6	99.9813%	0.018228
	Without e	2.3597×10^6	99.9796%	0.019028

TABLE 11. Optimized values and corresponding parameters.

	Optimized value	Corresponding parameters		
		Dimple diameter, d_0 (100 ~2000 μm)	Area ratio, S_p (5~30%)	Dimple depth, h_g (1 ~10 μm)
Friction force, $\bar{F}$ (dimensionless)	6.8500 (min)	N/A[a]	30	10
Load-carrying capacity, $\bar{W}$ (dimensionless)	513.0114 (max)	1883.389	5	5.805
Coefficient of friction, f	0.0506 (min)	1883.389	30	6.430

[a]N/A=No significant effect

very little. One possible explanation is that almost 99.73% of geometrical parameters are within three standard deviations of the mean, and since those manufacturing errors are so small, their influence is nil.

C. PARAMETERS OPTIMIZATION

Compared with the independent variables, the role of manufacturing errors is very small. In addition, manufacturing errors are random variables and very difficult to control. Therefore, manufacturing errors are not considered in the optimization process. The Nloptr library, which is an R interface, is used to attain nonlinear optimization.

To reach the best texture performance, optimized values of $\bar{F}$ and f are minimum values, and an optimized value of $\bar{W}$ is a maximum value. The results indicate that optimized values of $\bar{F}$, $\bar{W}$, and f call for different values of the dimple diameter, the area ratio, and the dimple depth when operating in a hydrodynamic lubrication regime (as given in Table 11).

The results reveal that a large dimple diameter yields a high texture performance regardless of performance parameters. A small value of the area ratio ($S_p = 5\%$) is required to attain a maximum value of the load-carrying capacity, and a large value ($S_p = 30\%$) is needed to attain minimum values of the friction force and the coefficient of friction. A value of the dimple depth in medium range ($h_g = 5.5\sim6.5\ \mu$m) can attain optimized values of the load-carrying capacity and the coefficient of friction, and a large value ($h_g = 10\ \mu$m) can attain optimized values of the friction force.

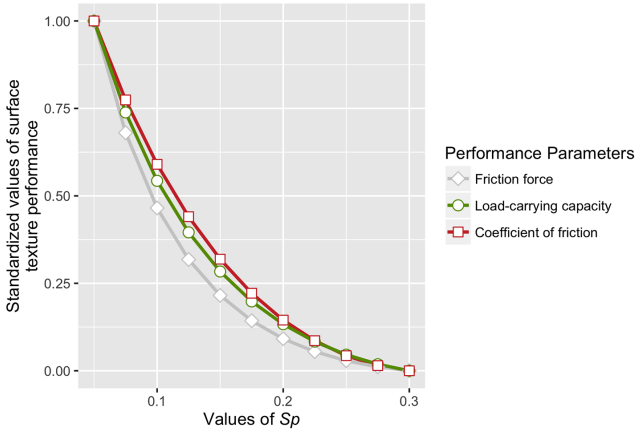

FIGURE 5. Standardized values of surface texture performance.

The coefficient of friction is more frequently used than the friction force. If only considering the load-carrying capacity and the coefficient of friction, an optimized value of performance calls for a large value of the dimple diameter and a median value of the dimple depth. However, it calls for different values of the area ratio. As a result, the area ratio may be a key parameter to balance the optimized value of the load-carrying capacity and the coefficient of friction. To investigate the impact of the area ratio, the predicted value is regenerated by the models without e. For this purpose, the dimple diameter is set at 1883.389 μm, the dimple depth is set at 6 μm, and the area ratio varied from 5% to 30%. The predicted values of the friction force, the load-carrying capacity, and the coefficient of friction are not comparable because their range is disparate. Therefore, the values are standardized, and the range is from 0 to 1 (as shown in Fig. 5). Along with the increase of the area ratio, both the load-carrying capacity and the coefficient of friction are decreased. Their curves are comparable, so the change of S_p leads to a similar varying tendency. Therefore, it is difficult to determine the area ratio to reach a relatively high load-carrying capacity and lower coefficient of friction. The design requirements will dictate which performance parameter is more important.

In summary, when the designer chooses the dimple diameter, the dimple depth, and the area ratio in the value range (100 ~2000 μm for the diameter, 1~10 μm for the depth, and 5~30% for the area ratio), he or she should first confirm which performance parameter is the most important. To obtain the optimized values of the friction force $\bar{F}$, the load-carrying capacity $\bar{W}$, or the coefficient of friction f, the following equations are solved:

$$Min\ \bar{F} = f\left(d_0, h_g, S_p\right) \tag{8}$$

$$Max\ \bar{W} = g\left(d_0, h_g, S_p\right) \tag{9}$$

$$Min\ f = h(d_0, h_g, S_p) \tag{10}$$

$$\text{Subject to: } \begin{cases} 100\mu\text{m} \le d_0 \le 2000\ \mu\text{m} \\ 1\ \mu\text{m} \le h_g \le 10\ \mu\text{m} \\ 5\% \le S_p \le 30\%. \end{cases} \quad (11)$$

The optimized value of friction force $\bar{F}$ calls for $h_g = 10\ \mu$m, $S_p = 30\%$.

The optimized value of load-carrying capacity $\bar{W}$ calls for $d_0 = 1883.389\ \mu$m, $h_g = 5.805\ \mu$m, $S_p = 5\%$.

The optimized value of coefficient of friction f calls for $d_0 = 1883.389\ \mu$m, $h_g = 6.430\ \mu$m, $S_p = 30\%$.

Generally, a design calls for the optimized values on all aspects of surface texture performance, but this is difficult to satisfy due to the intertwined relationships among the aspects of performance. For instance, if a design needs the optimal combinatorial performance in load-carrying capacity and the coefficient of friction, the dimple's diameter and its depth should be 1883 μm and 5.5∼6.5 μm, respectively, and the value of the area ratio should be determined depending on the design requirements.

D. COMPARISON WITH PHYSICAL EXPERIMENTAL RESULTS

In this section, we compare the results of this research with those of published experimental measurements. In separate research, Wang *et al.* [30] report an investigation of the optimized value of the load-carrying capacity of thrust bearings working in water lubrication. Their experiments use seven combinations of the geometrical parameters, including the dimple diameter (50∼650 μm), the dimple depth (2∼16.6 μm), and the area ratio (2.8∼22.5%). Several fixed levels of these parameters are determined. Results of the experiments show that dimples with the diameter at 350 μm, the depth at 3.2 μm, and the area ratio at 5% yield the best performance in terms of generating the load-carrying capacity. These findings are in accordance with the results of this research in terms of the area ratio. That is, a relatively small value of the area ratio yields a high level of load-carrying capacity. Their research uses multiple fixed levels of the geometrical parameters but only investigates one variable at a time without considering the interaction among other variables, which might bias the results.

Referring back to Fig. 3, the dimple's diameter and its depth have greater influence compared to the area ratio in terms of the load-carrying capacity and the coefficient of friction. Recall that the area ratio has the most influence compared to other factors in terms of the friction force. This finding agrees with the experimental evaluation of Yan *et al.* [26]. They carried out frictional tests on the textured specimens of cast iron with oil lubrication under the contact pressures of 0.2 and 1 MPa and sliding velocities of 0.1 and 0.5 m/s. However, they also find that the frictional performance is optimized when the dimple diameter is 100∼200 μm (range from 50 to 300 μm), the area ratio is 5∼10% (range from 5% to 20%), and the dimple depth is 10 μm (range from 5 μm to 20 μm). The findings are different from the results of this research. One of the possible reasons is that the operating conditions are different. Although they considered the interaction among variables, they also used fixed levels of variables and only tested some levels of the factorial design (16 levels among 64 levels), without considering the probability of each level.

Reference [31] uses the same value of working conditions under hydrodynamic lubrication as this research. They use the numerical optimization approach to determine the optimum texture shape for generating the highest load-carrying capacity. Their research reveals that chevron-type shapes and trapezoid-like shapes produce the highest load-carrying capacity. The result of optimization shows that the highest load-carrying capacity occurs at the area ratio of 49% for unidirectional sliding and at the area ratio of 63.5% for bidirectional sliding. The result is different than that of this research which suggests that a small area ratio (i.e., 5%) is needed to obtain great load-carrying capacity. One possible reason for the difference is that the shape of dimples is different. However, to reduce the contact area and stress concentration caused by surface texturing, research reported by Wang *et al.* [32] recommends that the area ratio be less than 20%. Simulation results of reference [31] show that the proposed optimum trapezoid-like shapes always have greater load-carrying capacity than the regular shapes at an area ratio of 30%. Thus, dimples with trapezoid-like shapes could be adopted in further research, and may obtain greater load-carrying capacity than circular dimples.

Another important explanation for the difference between results of this research and those of physical experiments is that this research uses the Reynolds model, which underestimates the cavitation effects. Cavitation is shown to have a significant influence on the performance of near-parallel textured contacts [33]. In order to address the cavitation effects, a mass-conservative algorithm proposed by Elrod and Adams [34] is adopted to study the behavior of micro-textured journal bearings [35], [36]. Comparisons between the mass-conservative algorithm and Reynolds model show that the Reynolds model largely underestimates the cavitation area and yields inaccuracies in the prediction of the load-carrying capacity. The Jakobsson–Floberg–Olsson (JFO) model, which enforces mass conservation, is another widely used cavitation model in hydrodynamic lubrication theory [37]. The prediction from the JFO model is more realistic than that from the Reynolds model, according to experimental and simulation results on parallel thrust bearings and journal bearings [38]–[40]. Modifications of computational algorithms that incorporate the JFO model are proposed to conserve mass continuity, improve numerical instability, and overcome convergence issues [41]. Adopting the JFO model and its modifications in numerical experiments probably increases the model complexity, but it enhances the accuracy of prediction.

VII. CONCLUSIONS

Compared with previous studies, this study adopts a general procedure for quantifying uncertainty in the analysis

of textured surfaces operating in the hydrodynamic lubrication regime. The statistical method in this research generally solves the problems of quantifying uncertainty, mixed uncertainty, and generalization of uncertainty mentioned above. As to the problem of quantifying uncertainty, the study considers the probability of each level and adopts a normal distribution to represent the multiple levels of uncertain parameters. As to the mixed uncertainty from multiple sources, the study considers three variables at a time and investigates the interaction among these variables. As to the generalization of uncertainty, the study uses a numerical experiment and the statistical method to simulate the uncertainty of the manufacturing process. These methods can be generalized to other manufacturing processes and operating conditions by adjusting model parameters. This study investigates a general way of quantifying uncertainty from multiple sources.

The following conclusions can be drawn from the results of this investigation.

1) The statistical models can explain and predict the influence of texture dimensions with uncertainty on the performance of surface textures. The logarithmic models can explain more than 99.98% of the variance in data, and they are verified to be robust among different data samples.
2) The statistical models indicate that the most critical geometric parameter for the coefficient of friction and the load-carrying capacity is the dimple diameter, whereas the most critical geometric parameter for the friction force is the area ratio. Manufacturing errors that follow the normal distribution with three sigma quality are not significant.
3) The dimple diameter of 1883 μm is optimal to generate a low friction force, a high load-carrying capacity, and a low coefficient of friction. The dimple depth of 5.5$\sim$6.5 μm is optimal for a high load-carrying capacity and a low coefficient of friction. The area ratio should be determined based on the importance degree of the load-carrying capacity and the coefficient of friction.

REFERENCES

[1] D. Gropper, L. Wang, and T. J. Harvey, "Hydrodynamic lubrication of textured surfaces: A review of modeling techniques and key findings," *Tribol. Int.*, vol. 94, pp. 509–529, Feb. 2016.

[2] R. B. Siripuram, "Analysis of hydrodynamic effects of microasperity shapes on thrust bearing surfaces," M.S. thesis, Dept. Mech. Eng., Univ. Kentucky, Lexington, KY, USA, 2003.

[3] D. G. Coblas, A. Fatu, A. Maoui, and M. Hajjam, "Manufacturing textured surfaces: State of art and recent developments," *Proc. Inst. Mech. Eng., J. J. Eng. Tribol.*, vol. 229, no. 1, pp. 3–29, 2015.

[4] I. Etsion, "State of the art in laser surface texturing," *J. Tribol.*, vol. 127, no. 1, pp. 248–253, 2005.

[5] C. Ma and H. Zhu, "An optimum design model for textured surface with elliptical-shape dimples under hydrodynamic lubrication," *Tribol. Int.*, vol. 44, no. 9, pp. 987–995, 2011.

[6] I. Etsion, Y. Kligerman, and G. Halperin, "Analytical and experimental investigation of laser-textured mechanical seal faces," *Tribol. Trans.*, vol. 42, no. 3, pp. 511–516, 1999.

[7] N. Ren, T. Nanbu, Y. Yasuda, D. Zhu, and Q. Wang, "Micro textures in concentrated-conformal-contact lubrication: Effect of distribution patterns," *Tribol. Lett.*, vol. 28, no. 3, pp. 275–285, 2007.

[8] T. Ibatan, M. S. Uddin, and M. A. K. Chowdhury, "Recent development on surface texturing in enhancing tribological performance of bearing sliders," *Surface Coatings Technol.*, vol. 272, pp. 102–120, Jun. 2015.

[9] Y. Gao, B. Wu, Y. Zhou, and S. Tao, "A two-step nanosecond laser surface texturing process with smooth surface finish," *Appl. Surface Sci.*, vol. 257, no. 23, pp. 9960–9967, 2011.

[10] G. Bonori and F. Pellicano, "Non-smooth dynamics of spur gears with manufacturing errors," *J. Sound Vibrat.*, vol. 306, no. 1, pp. 271–283, 2007.

[11] A. Bodas and A. Kahraman, "Influence of carrier and gear manufacturing errors on the static load sharing behavior of planetary gear sets," *JSME Int. J. Ser. C, Mech. Syst., Mach. Elements Manuf.*, vol. 47, no. 3, pp. 908–915, 2004.

[12] H. Ligata, A. Kahraman, and A. Singh, "An experimental study of the influence of manufacturing errors on the planetary gear stresses and planet load sharing," *J. Mech. Design*, vol. 130, no. 4, 2008, Art. no. 041701.

[13] K. N. Otto and E. K. Antonsson, "Tuning parameters in engineering design," *J. Mech. Design*, vol. 115, no. 1, pp. 14–19, 1993.

[14] K. L. Wood and E. K. Antonsson, "Computations with imprecise parameters in engineering design: Background and theory," *J. Mech., Transmiss., Auto. Design*, vol. 111, pp. 616–625, Jun. 1989.

[15] K. Otto and C. Jacobson, "Using model uncertainty to reduce verification and validation in noise and vibration problems," in *Proc. Int. Design Eng. Tech. Conf. Comput. Inf. Eng. Conf. (ASME)*, 2012, pp. 335–346.

[16] A. Parkinson, "Robust mechanical design using engineering models," *J. Vibrat. Acoust.*, vol. 117, pp. 48–54, Jun. 1995.

[17] M. Barkallah, J. Louati, and M. Haddar, "Evaluation of manufacturing tolerance using a statistical method and experimentation," *Int. J. Simul. Model.*, vol. 11, no. 1, pp. 5–16, 2012.

[18] F. Puh, Z. Jurkovic, M. Perinic, M. Brezocnik, and S. Buljan, "Optimization of machining parameters for turning operation with multiple quality characteristics using Grey relational analysis," *Tehnički vjesnik*, vol. 23, pp. 377–382, Apr. 2016.

[19] B. S. Prasad and M. P. Babu, "Correlation between vibration amplitude and tool wear in turning: Numerical and experimental analysis," *Eng. Sci. Technol., Int. J.*, vol. 20, no. 1, pp. 197–211, 2017.

[20] C. Siyu, T. Jinyuan, L. Caiwang, and W. Qibo, "Nonlinear dynamic characteristics of geared rotor bearing systems with dynamic backlash and friction," *Mech. Mach. Theory*, vol. 46, no. 4, pp. 466–478, 2011.

[21] M. Byrtus and V. Zeman, "On modeling and vibration of gear drives influenced by nonlinear couplings," *Mech. Mach. Theory*, vol. 46, no. 3, pp. 375–397, 2011.

[22] H. Moradi and H. Salarieh, "Analysis of nonlinear oscillations in spur gear pairs with approximated modelling of backlash nonlinearity," *Mech. Mach. Theory*, vol. 51, pp. 14–31, May 2012.

[23] G. Ryk, Y. Kligerman, and I. Etsion, "Experimental investigation of laser surface texturing for reciprocating automotive components," *Tribol. Trans.*, vol. 45, no. 4, pp. 444–449, 2002.

[24] A. Kovalchenko, O. Ajayi, A. Erdemir, G. Fenske, and I. Etsion, "The effect of laser surface texturing on transitions in lubrication regimes during unidirectional sliding contact," *Tribol. Int.*, vol. 38, no. 3, pp. 219–225, 2005.

[25] L. Galda, P. Pawlus, and J. Sep, "Dimples shape and distribution effect on characteristics of Stribeck curve," *Tribol. Int.*, vol. 42, no. 10, pp. 1505–1512, 2009.

[26] D. Yan, N. Qu, H. Li, and X. Wang, "Significance of dimple parameters on the friction of sliding surfaces investigated by orthogonal experiments," *Tribol. Trans.*, vol. 53, no. 3, pp. 703–712, 2010.

[27] W. Grabon, W. Koszela, P. Pawlus, and S. Ochwat, "Improving tribological behaviour of piston ring–cylinder liner frictional pair by liner surface texturing," *Tribol. Int.*, vol. 61, pp. 102–108, May 2013.

[28] D. C. Montgomery, *Design and Analysis of Experiments*, vol. 6. New York, NY, USA: Wiley 2002.

[29] A. Dean and D. Voss, *Design and Analysis of Experiments*. New York, NY, USA: Speringer-Verlag, 1999.

[30] X. Wang, K. Kato, K. Adachi, and K. Aizawa, "Loads carrying capacity map for the surface texture design of SiC thrust bearing sliding in water," *Tribol. Int.*, vol. 36, no. 3, pp. 189–197, 2003.

[31] C. Shen and M. Khonsari, "Numerical optimization of texture shape for parallel surfaces under unidirectional and bidirectional sliding," *Tribol. Int.*, vol. 82, pp. 1–11, Feb. 2015.

[32] X. Wang, J. Wang, B. Zhang, and W. Huang, "Design principles for the area density of dimple patterns," *Proc. Inst. Mech. Eng., J, J. Eng. Tribol.*, vol. 229, no. 4, pp. 538–546, 2015.
[33] M. Dobrica, M. Fillon, M. Pascovici, and T. Cicone, "Optimizing surface texture for hydrodynamic lubricated contacts using a mass-conserving numerical approach," *Proc. Inst. Mech. Eng., J, J. Eng. Tribol.*, vol. 224, no. 8, pp. 737–750, 2010.
[34] H. Elrod and M. Adams, "A computer program for cavitation and starvation problems," *Cavitation Rel. Phenomena Lubricat.*, pp. 37–41, 1974.
[35] R. Ausas, P. Ragot, J. Leiva, M. Jai, G. Bayada, and G. C. Buscaglia, "The impact of the cavitation model in the analysis of microtextured lubricated journal bearings," *J. Tribol.*, vol. 129, pp. 868–875, Oct. 2007.
[36] M. Fesanghary and M. M. Khonsari, "On self-adaptive surface grooves," *Tribol. Trans.*, vol. 53, no. 6, pp. 871–880, 2010.
[37] J. Zhang and Y. Meng, "Direct observation of cavitation phenomenon and hydrodynamic lubrication analysis of textured surfaces," *Tribol. Lett.*, vol. 46, no. 2, pp. 147–158, 2012.
[38] Y. Qiu and M. M. Khonsari, "On the prediction of cavitation in dimples using a mass-conservative algorithm," *J. Tribol.*, vol. 131, no. 4, p. 041702, 2009.
[39] C. Shen and M. M. Khonsari, "On the magnitude of cavitation pressure of steady-state lubrication," *Tribol. Lett.*, vol. 51, no. 1, pp. 153–160, 2013.
[40] C. Shen and M. M. Khonsari, "Effect of dimple's internal structure on hydrodynamic lubrication," *Tribol. Lett.*, vol. 52, no. 3, pp. 415–430, 2013.
[41] M. Fesanghary and M. M. Khonsari, "A modification of the switch function in the Elrod cavitation algorithm," *J. Tribol.*, vol. 133, no. 2, p. 024501, 2011.

FAN MO received the B.S. degree in industrial engineering from Chongqing University, Chongqing, China, in 2015, where he is currently pursuing the M.S. degree in management science and engineering. He has authored or co-authored four research publications, including three journal papers. His research interest includes applied statistical analysis, human–computer interaction, interface design for mobile and wearable devices, and social network analysis. He was a Session Chair of the International Conference on Human–Computer Interaction in 2016.

CONG SHEN received the Ph.D. degree in mechanical engineering from Louisiana State University, Baton Rouge, LA, USA, in 2016. He has authored or co-authored several research publications. His research interest includes tribology, machinery performance analysis, and numerical analysis.

JIA ZHOU received the B.S. degree in industrial engineering from Tongji University, Shanghai, China, in 2007, and the Ph.D. degree from the Institute of Human Factors and Ergonomics, Tsinghua University, Beijing, China, in 2013. From 2011 to 2012, she was a Visiting Scholar with the Trace Research and Development Center, University of Wisconsin–Madison, Madison, WI, USA. Since 2013, she has been an Assistant Professor with the Industrial Engineering Department, Chongqing University, Chongqing, China. She has authored or co-authored 18 research publications, including 11 journal papers. Her main research deals with applied statistical analysis, human–computer interaction, universal design, technology acceptance, usability engineering, interface design for mobile devices, and accessibility. Dr. Zhou was offered an appointment as an Honorary Associate at the Trace Research and Development Center for her contributions to the research project. She is a Reviewer of the ACM SIGCHI Conference on Human Factors in Computing Systems and the Session Chair of the International Conference on Human–Computer Interaction.

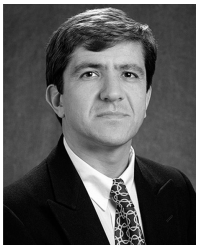

MICHAEL M. KHONSARI received the B.S, M.S, and Ph.D. degrees in mechanical engineering from The University of Texas at Austin, Austin, TX, USA. He was a Faculty Member with The Ohio State University and the University of Pittsburgh for a number of years. From 1984 to 1988, he was a Professor with The Ohio State University. He served as the Chairman of the Department of Mechanical Engineering and Energy Processes, Southern Illinois University. He is a Dow Chemical Endowed Chair and a Professor and the Director of the Center for Rotating Machinery, Department of Mechanical Engineering, Louisiana State University, Baton Rouge, LA, USA. He has authored several books. He has also served as a Research Faculty Fellow with the NASA Lewis (now Glenn) Research Center, Wright-Patterson Air Force Laboratories, and the U.S. Department of Energy. His research interests include tribology (friction, lubrication, and wear), machinery performance analysis, numerical analysis, and heat transfer. He is known for his research in tribology and, in particular, application of thermodynamic methods in tribology. Dr. Khonsari is a Fellow of the ASME. He was the recipient of the ASME Burt L. Newkirk Award, the STLE Presidential Award, the Alcoa Foundation Award, and the William Kepler Whiteford Faculty Fellow Award from the University of Pittsburgh.